Australasian Physical & Engineering Sciences in Medicine (2019) 42:921–938
https://doi.org/10.1007/s13246-019-00790-1

SCIENTIFIC PAPER

Analysis of brain functional connectivity network in MS patients constructed by modular structure of sparse weights from cognitive task-related fMRI

Seyedeh Naghmeh Miri Ashtiani[1] · Hamid Behnam[1] · Mohammad Reza Daliri[1] · Gholam-Ali Hossein-Zadeh[2,3] · Masoud Mehrpour[4]

Received: 18 February 2019 / Accepted: 12 August 2019 / Published online: 26 August 2019

Abstract

Cognitive dysfunction in multiple sclerosis (MS) seems to be the result of neural disconnections, leading to a wide range of brain functional network alterations. It is assumed that the analysis of the topological structure of brain connectivity network can be used to assess cognitive impairments in MS disease. We aimed to identify these brain connectivity pattern alterations and detect the significant features for the distinction of MS patients from healthy controls (HC). In this regard, the importance of functional brain networks construction for better exhibition of changes, inducing the improved reflection of functional organization structure should be precisely considered. In this paper, we strove to introduce a framework for modeling the functional connectivity network by considering the two most important intrinsic sparse and modular structures of brain. For the proposed approach, we first derived group-wise sparse representation via learning a common over-complete dictionary matrix from the aggregated cognitive task-based functional magnetic resonance imaging (fMRI) data of all subjects of the two groups to be able to investigate between-group differences. We then applied the modularity concept on achieved sparse coefficients to compute the connectivity strength between the two brain regions. We examined the changes in network topological properties between relapsing–remitting MS (RRMS) and matched HC groups by considering the pairwise connections of regions of the resulted weighted networks and extracting graph-based measures. We found that the informative brain regions were related to their important connectivity weights, which could distinguish MS patients from the healthy controls. The experimental findings also proved the discrimination ability of the modularity measure among all the global features. In addition, we identified such local feature subsets as eigenvector centrality, eccentricity, node strength, and within-module degree, which significantly differed between the two groups. Moreover, these nodal graph measures have been served as the detectors of brain regions, affected by different cognitive deficits. In general, our findings illustrated that integration of sparse representation, modular structure, and pairwise connectivity strength in combination with the graph properties could help us with the early diagnosis of cognitive alterations in the case of MS.

Keywords Cognitive dysfunction · Multiple sclerosis (MS) disease · Cognitive task-based fMRI · Sparse representation · Modular structure · Discriminative network properties

Electronic supplementary material The online version of this article (https://doi.org/10.1007/s13246-019-00790-1) contains supplementary material, which is available to authorized users.

✉ Mohammad Reza Daliri
daliri@iust.ac.ir

[1] Biomedical Engineering Department, School of Electrical Engineering, Iran University of Science and Technology (IUST), Tehran, Iran

[2] School of Cognitive Sciences (SCS), Institute for Research in Fundamental Sciences (IPM), Tehran, Iran

[3] Control and Intelligent Processing Center of Excellence, School of Electrical and Computer Engineering, University College of Engineering, University of Tehran, Tehran, Iran

[4] Department of Neurology, Firoozgar Hospital, Tehran University of Medical Sciences, Tehran, Iran

Introduction

Multiple sclerosis (MS) is an inflammatory demyelination and an autoimmune disease of the central nervous system (CNS), which can lead to a wide range of signs and symptoms. Cognitive impairment is one of the common symptoms in patients with MS, affecting different domains such as working memory, attention and decision-making, verbal and visual memory, information processing speed, and executive functions [1–3]. Dysfunction of cognitive abilities in MS seems to be the result of damage to white matter (WM) connections or cortical associated areas. This hypothesis can be investigated with an accurate quantitative description of topological structure of brain connectivity [4–7].

It is believed that human brain, as a complex network comprising a large number of elements that interact functionally with each other to exchange information efficiently, can be represented as a graph. The brain regions are defined as nodes (elements), and the pairwise functional connectivity can determine the edges [8, 9]. In recent years, many studies have demonstrated the potential of functional brain network based on functional magnetic resonance imaging (fMRI) data for the detection of alterations in brain connectivity patterns and also the identification of reliable markers for various brain disorders both in the early stages and during the progression of diseases [2, 10–13]. Thus, the construction of brain functional networks is a substantial step for better understanding of brain activation changes in different conditions [14–16]. To date, a large number of approaches have been employed for functional brain network modelling. Pearson's correlation is one the most common approaches, which has been broadly used to define the functional connectivity of brain areas [2, 10, 13, 17–21]. Gamboa et al. [2] conducted the first study to assess the modularity abnormalities of Pearson correlation based-functional networks with resting-state (rs-fMRI) data in MS patients compared to controls. Although Pearson's correlation is easy to implement, it only captures the pairwise relationship strength without considering the contribution of other brain regions [22, 23].

Independent component analysis (ICA) has also been widely applied to fMRI data to construct functional brain network by separating independent components temporally or spatially [24, 25]. The relevance between cognitive impairments and changes in default mode network (DMN) connectivity at rest in MS was assessed through ICA by Bonavita et al. [7]. The results were consistent with the findings reported by Rocca et al. [26] and Roosendaal et al. [27]. They assessed the between-group differences in DMN functional connectivity and observed significantly reduced activity in the anterior cingulate cortex (ACC) in cognitively impaired patients with MS. However, a number of recent studies have claimed that the independence of distinct activity patterns that occur simultaneously is not guaranteed by independence assumption in ICA algorithm [24, 28, 29]. Instead, according to biological findings, they have suggested that the idea of sparsity in the determination of neural activities is more effective than independency [28, 30–32]. To overcome these drawbacks, a data-driven fMRI analysis approach was introduced based on sparse representation, which can regard each brain region's time series as a linear integration of sparse set of dynamic components with different temporal patterns. The constructed brain network based on sparse representation method was supported by the assumption that the brain regions only directly interact with a few other regions [33]. It is worth noting that sparse signal representation approaches have highly been regarded by recent works to construct brain network for such brain disorders as Alzheimer's disease (AD) [34].

Since brain network has many different intrinsic structures, considering only the sparsity for functional brain network modelling cannot be sufficient to accurately describe the topological structure of brain connectivity. Given that the modular architecture is one of the most important intrinsic brain properties [15], several recent frameworks imposed group structure term into the models for the construction of functional brain network in order to facilitate the understanding of human brain function [22, 23, 35–37]. Therefore, one of the major issues in the study of functional connectivity networks is the characterization of modular (community) structure in networks, by detecting densely interconnected groups of nodes with sparsely between-groups connections [38, 39].

Yu et al. [23] optimized the network modeling by adding a group structure-based constraint with the consideration of connectivity strength derived from Pearson's correlation and sparsity for mild cognitive impairment (MCI) classification. Wang et al. [22] also introduced a new model by merging sparse and low-rank constraints to retain the modular structure of brain networks. The proposed sparse low-rank model improved the classification performance of patients with depression and controls using optimal eight graph-based features.

Considering the limitations and challenges facing functional brain network construction, we aim to propose a method for functional network modeling using modular structure concept based on an efficient group-wise sparse representation through learning a common dictionary from aggregated regional cognitive task-related fMRI signals of all subjects in two groups. Therefore, the connectivity strength weight of the two brain regions are yielded with the consideration of the influence of other regions and the

integration of both important brain network properties of sparsity and modularity. Based on our approach, we expect that the constructed functional connectivity networks are more reasonable and the connectivity strength of the two brain regions could better reflect the different functional configurations. In addition, in our recent study, the ability of graph-based properties from different aspects for the investigation of topological differences caused by structural lesions in the brain of MS patients in comparison with the healthy controls was confirmed [13]. Accordingly, we also extract various graph measures from weighted functional networks to validate our method.

The rest of this paper is organized as follows. In "Materials and methods" section, we will describe the materials and methods including a briefly description of fMRI data acquisition during a specific cognitive task performance, dictionary learning and sparse representation theory. We will detail the proposed method for functional connectivity network construction. "Results" section will illustrate the results of the proposed method. We will present the discussions in "Discussion", followed by our conclusion in "Conclusion" section.

Materials and methods

Participants and task-based fMRI data acquisition

Eight right-handed RRMS patients in the early stages of disease (mean age 36.25 ± 8.43 ranging from 26 to 44 years, 7 female), and twelve healthy controls (mean age 30.67 ± 4.81 ranging from 23 to 40 years, 8 female) were included in our study. The patients with the disease diagnosis of less than 5 years and minimal physical disability, determined by Expanded Disability Status Scale (i.e., EDSS < 3.5), were selected by neurologist from Firoozgar hospital, Tehran, Iran. An informed consent was obtained from each subject before the implementation of the study.

Before the scan, every MS patient was assessed using some neuropsychological tests at Pars hospital in Tehran, Iran. These behavioral assessments included: Wechsler memory scale-revised (WMS-R), Block Design and Symbol Digit subtests of the WAIS-R (Wechsler adult intelligence scale-revised) [40], and Stroop test [41] to evaluate attentional skills, full memory and verbal memory functions. The patients with MS had full memory scores between 67 and 112 (mean score 92.25 ± 13.32), verbal memory scores ranging from 65 to 103 (mean score 90.37 ± 11.81), a range score of 91–121 (mean score 102.37 ± 12.38) for the attention/construction index, and auditory attention scores between 4 and 10 (mean score 6.37 ± 1.92).

The Paced Auditory Serial Additional Task (PASAT) has been frequently used to evaluate cognitive functions in various neurological disorders. The importance and efficiency of PASAT for the detection of cognitive impairments was also suggested by research studies for a variety of neurological syndromes such as MS. The PASAT is recognized as a measure of multiple functional domains as it requires the successful completion of a variety of cognitive functions including working memory, attention, and the speed of information processing [3, 42].

Each subject performed a Persian version of the modified PASAT during the fMRI scan. The PASAT task included six activation blocks, each activation block of 30 s was alternated with the resting block of 30 s. Every auditory stimulus of a random series of digits between 1 and 9 was presented every 3 s during each activation block. The participants were requested to add the two last numbers immediately after hearing the last number and were expected to answer by comparing it with the target number using a response box.

The functional MR images were acquired on a 3.0T Siemens Tim Trio MRI scanner at the Imam Khomeini hospital, Tehran, Iran. fMRI scans were obtained through echo planar imaging (EPI) sequence, with repetition time (TR) = 2000 ms, echo time (TE) = 30 ms, field of view (FOV) = 192 mm^2, flip angle = 90°, matrix size = 64 × 64, voxel size = 3 × 3 × 4mm^3, 30 slices per volume, slice thickness = 4 mm, and 180 vols. The structural images were acquired using a high resolution three dimensional T1-weighted magnetization-prepared rapid gradient-echo (MP-RAGE) sequence, with TR = 1.80 s, TE = 3.44 ms, flip angle = 7°, matrix size = 256 × 256, voxel size = 1 × 1 × 1mm^3, and 176 sagittal slices with thickness of 1 mm.

Data pre-processing

FSL toolbox from the FMRIB's Software Library (www.fmrib.ox.ac.uk/fsl) [43–45] was used for all the pre-processing steps. The pre-processing stage was conducted as follows: the elimination of extracranial tissues using brain extraction tool (BET) [46], discarding the first 5 EPI volumes for scanner stabilization, the head motion correction via MCFLIRT [47], spatial smoothing through a 6-mm^3 full-width at half-maximum (FWHM) Gaussian kernel, high-pass temporal filtering with a cutoff of 0.01 Hz, the co-registration of functional images on structural image, and the normalization into the Montreal Neurological Institute (MNI) 152 standard space through FMRIB's linear image registration tool (FLIRT) [48].

More details about clinical information of MS patients, task paradigm and fMRI data pre-processing steps are cited in Ashtiani et al. [13].

Dictionary learning and sparse representation of task-related fMRI signals

In this study, we applied dictionary learning and sparse signal representation as a new tool for fMRI data analysis to improve the identification of brain connectivity pattern alterations and to detect the reliable markers in the early phases of MS disease. The sparse signal coding from an over-complete dictionary can effectively factorize each fMRI time series based on a linear integration of a limited number of relevant dictionary atoms [30, 36, 49–51]

For each subject from the two groups (i.e., HC and MS), the first step was to extract fMRI time series on all voxels, which were normalized into the standard Montreal Neurological Institute (MNI) space. Then, we parcellated each subject's brain into 116 regions of interest (ROIs) according to the Automated Anatomical Labeling (AAL) atlas [52] and determined the regional time course by averaging fMRI signals of all voxels in each ROI. After the normalization of representative time series to zero mean and standard deviation 1, the data matrix of a subject was defined as signal matrix $S_k \in \mathbb{R}^{t\times n}$, where t is the number of temporal samples and n denotes the number of ROIs. Eventually, all obtained data matrices of all subjects from the two groups were aggregated into a big signal set $\boldsymbol{S} \in \mathbb{R}^{t\times N}$, where the dimension of N vector is $x \times n$, in which x demonstrates the total number of subjects $= \left[S_{G_{HC}}, S_{G_{MS}}\right]$. The task-related fMRI signal set $\boldsymbol{S}$ is modeled as linear regression terms by employing the online dictionary learning and sparse coding algorithm in Mairal et al. [53], based on a common over-complete dictionary matrix $D \in \mathbb{R}^{t\times m}$(i.e.,$m > t$) and a weight coefficient matrix $\boldsymbol{\alpha} \in \mathbb{R}^{m\times N}$ for sparse representation (i.e.,$\boldsymbol{S} = D \times \boldsymbol{\alpha} + \boldsymbol{\varepsilon}$), where m and $\boldsymbol{\varepsilon}$ denote the number of dictionary atoms and representation error (noise), respectively. The coefficient matrix $\boldsymbol{\alpha}$ is composed of $\alpha_{G_{HC}}$ and $\alpha_{G_{MS}}$, which is in accordance with the group organization and regional arrangement of signal matrix $\boldsymbol{S}$. Specifically, each atomic signal in the learned dictionary D represents the functional brain network activities, and its corresponding sparse coefficients express the ROIs' spatial distribution of this dictionary atom.

Since the learned dictionary D is the same across all subjects, we are able to compare the functional networks in the group-level to identify the inter-group differences in various brain conditions.

In summary, the optimization problem of dictionary learning and sparse representation can be formulated as follows: l_1 regularizes the optimization problem in Eq. (1) [53]:

$$C \triangleq \left\{ D \in \mathbb{R}^{t\times m}\, s.t. \forall j = 1, \ldots m,\ d_j^T d_j \le 1 \right\}$$
$$\min_{D\in C, \boldsymbol{\alpha}\in\mathbb{R}^{m\times N}} \frac{1}{2} \|S - D\boldsymbol{\alpha}\|_F^2 + \lambda \|\boldsymbol{\alpha}\|_{1,1} \tag{1}$$

The regularization parameter λ is known to balance the goodness-of-approximation and sparsity level. Also, the constraint on dictionary atoms $d_1, d_2, \ldots, d_m$, which is expressed by Eq. (1) is to avoid arbitrarily large values. In addition, the weight coefficients matrix can be converted into positive coefficients by adding non-negativity constraints to $\boldsymbol{\alpha}$ matrix.

Finally, each regional time series from a subject was determined by the learned dictionary, which had common atomic time course for all subjects of the two groups, and the associated sparse weights (Eq. (2)):

$$\begin{aligned} \boldsymbol{S} : \left[S_{HC_1}, \ldots, S_{HC_{x1}}, S_{MS_1}, \ldots, S_{MS_{x2}}\right] \\ = D \times \boldsymbol{\alpha} : \left[\alpha_{HC_1}, \ldots, \alpha_{HC_{x1}}, \alpha_{MS_1}, \ldots, \alpha_{MS_{x2}}\right] \end{aligned} \tag{2}$$

Identification of task related and anti-task related network components

After decomposing the fMRI signal to the sparse dictionary atoms, we aimed to reveal the brain network components within the learned dictionary, which indicated task-related and anti-task related dynamics for the detection of brain regions involving PASAT task function. According to the proposed method in Lv et al. [54], we tested both temporal and frequency characteristics of atomic signals to extract task-related/anti-task-related dictionary atoms. Thus, by computing the Pearson correlation between each dictionary atom and blocked task design convolved by canonical hemodynamic response function (HRF), we chose the atoms that showed the highest correlation with the stimulus paradigm [30, 54]. Some of these selected atoms were positively correlated with task design, and some others followed the stimulus pattern inversely, which could be considered as task-related and anti-task-related network components, respectively.

In addition, for the evaluation of the frequency characteristics of each atomic signal, we initially calculated the stimulus frequency for the PASAT task paradigm by Eq. (3):

$$\begin{aligned} f_{PASAT} &= \frac{1}{length\ of\ activiation\ phase + length\ of\ resting\ phase} \\ &= \frac{1}{(30+30)} = 0.0167Hz \end{aligned} \tag{3}$$

Then, we obtained the frequency spectrum of each dictionary atom to calculate the energy concentration of f_{PASAT} (i.e., $E_{f_{PASAT}}$) as a ratio between the energy of stimulus pattern frequency and the energy of all range of frequency values. A larger value of $E_{f_{PASAT}}$ indicated that the corresponding dictionary atom could be introduced as the representative of the task/anti-task related network components. Therefore, we selected the best network components of the common learned dictionary, which was in accordance with the task and anti-task based on both high correlations and larger value of $E_{f_{PASAT}}$. Afterward, the T-value was measured on

the weight coefficient of each ROI over all individual subjects of each group for the selected components (is defined as Eq. (4)). The $\boldsymbol{\alpha}_{G_l}(i,j)$ in Eq. (4) indicates the coefficient matrix of each group of HC or MS, which contains the sparse coefficient value of the jth ROI to the ith atomic component in the common dictionary. There, L shows the number of subjects in each group, and l demonstrates the group category. By transforming the obtained T-value to the z-score [55], we employ z-thresholded > 1.65 ($P < 0.05$) to extract the corresponding AAL-based spatial distribution in the group level. The results are shown in the "Results" section.

$$T(i,j) = \frac{\overline{\boldsymbol{\alpha}_{G_l}(i,j)}}{\sqrt{\frac{var\left(\boldsymbol{\alpha}_{G_l}(i,j)\right)}{L}}},\ \left(L = 1,2,\ldots,x_l\right),\ (l = HC\ or\ MS)$$
$$\overline{\boldsymbol{\alpha}_{G_l}(i,j)} = \frac{1}{L}\sum_{L=1}^{x_l}\boldsymbol{\alpha}_L(i,j),\ var\left(\boldsymbol{\alpha}_{G_l}(i,j)\right) = \frac{1}{L}\sum_{L=1}^{x_l}\left(\boldsymbol{\alpha}_L(i,j) - \overline{\boldsymbol{\alpha}_{G_l}(i,j)}\right)^2 \tag{4}$$

We determined the number of dictionary atoms and λ experimentally. We examined a range of various dictionary numbers from 200 to 500 with a step size of 100. Eventually, the 400 dictionary atoms were chosen according to the obtained results. This was due to the fact that this size of dictionary tends to be more satisfactory in terms of signal-to-noise, reconstruction residual, obtain larger values of $E_{f_{PASAT}}$ and correlation coefficient, which resulted in finding the best components related to the task and anti-task. Also, λ was set to 0.15 to provide accurate approximation, which was in compromise with the level of sparsity.

Functional connectivity network constructed by modular structure of sparse weights

In order to identify the alterations in network properties between MS and controls during a cognitive task performance, we considered the following principal concepts to propose our method for the construction of connectivity networks:

(1) The sparse coding idea of the neural activities, frequently suggested as a result of neuroscience findings [24, 28, 29].
(2) The construction of brain functional network through a model that can obtain pairwise relationship strength between the two brain regions with regard to the influence of other regions [22, 23].
(3) The modular (community) structure of the brain functional connectivity network is one of the most significant intrinsic structures, derived from two points of view: the first is the ability of the brain to carry out the specialized processing within the densely interconnected modules of areas, and the second is the brain's efficiency to accelerate the transfer of specialized information between different modules [15].

Consequently, we proposed our computational framework based on three important characteristics of 'sparsity', 'functional connectivity strength between the two regions with the consideration of the influence of all other areas', and 'modular architecture' to construct a functional connectivity network. We named our method the modular structure of sparse weights (MSPW), which could be used to construct a functional connectivity network.

The human brain is regarded as a complex network, which is denoted by a large set of elements that contribute functionally with each other [2, 8, 15, 56]. In this study, we applied AAL atlas brain parcellation to define these elements and our proposed MSPW method to obtain inter-regional functional connectivity. The MSPW approach involves the following steps to compute the pairwise connectivity strength. First, the online dictionary learning and the sparse coding method [47] were utilized for the aggregated task-based fMRI signals of all subjects from the two groups. This has been used to take the idea of sparsity structure of the neural activities into account, which is supported by neuropsychological results [24, 28, 29]. Based on this method, each ROI signal was represented by a linear combination of a sparse set of common dictionary atoms (Eq. (5)), where each atomic component had different temporal-frequency pattern. Next, the weighted functional connectivity network was constructed by the sum of pairwise multiplication of sparse coefficients corresponding to each region for each subject, as shown in Eq. (6). All the self-connections of the connectivity matrix were set to zero.

$$S_k = D \times \alpha_k : \begin{cases} ROI_1 : \alpha_{11}d_1 + \alpha_{21}d_2 + \cdots + \alpha_{m1}d_m \\ ROI_2 : \alpha_{12}d_1 + \alpha_{22}d_2 + \cdots + \alpha_{m2}d_m \\ ROI_N : \alpha_{1N}d_1 + \alpha_{2N}d_2 + \cdots + \alpha_{mN}d_m \end{cases}, \left(k = HC_1,\ldots,HC_{x_1}\ or\ MS_1,\ldots,MS_{x_2}\right) \tag{5}$$

$$C_{k_{1,2}} = \left(\alpha_{11} \cdot \alpha_{12}\right) + \left(\alpha_{21} \cdot \alpha_{22}\right) + \cdots + \left(\alpha_{m1} \cdot \alpha_{m2}\right) = \sum_{i=1}^{i=m} \left(\alpha_{i1} \cdot \alpha_{i2}\right)$$

$$\rightarrow C_{k_{n_1,n_2}} = \sum_{\substack{i=1 \\ n_1,n_2 \in \{1,\ldots,N\} \\ n_1 \neq n_2}}^{i=m} \left(\alpha_{in_1} \cdot \alpha_{in_2}\right) \rightarrow Connectivity_k = \begin{bmatrix} 0 & \cdots & C_{1,N} \\ \vdots & \ddots & \vdots \\ C_{N,1} & \cdots & 0 \end{bmatrix} \tag{6}$$

We used this approach to follow two purposes:

(1) We obtained the pairwise connectivity strength by considering the influence of other regions, because the resulted sparse coefficients for each subject were achieved based on a common learned dictionary with the presence of all regional fMRI time series and,
(2) This method considered the modular structure for the construction of a connectivity network. This could be due to the fact that those regions involved in common specialized processing might be expressed on the basis of similar dictionary atoms with relatively high overlaps. Thus, the pairwise multiplication of the sparse coefficients of these regions can lead to a stronger connection. It is possible to prove this assumption based on the obtained results from activated brain regions related to task or anti-task. For example, the areas involving anti-task exhibited stronger connections with each other. However, the connection strength between

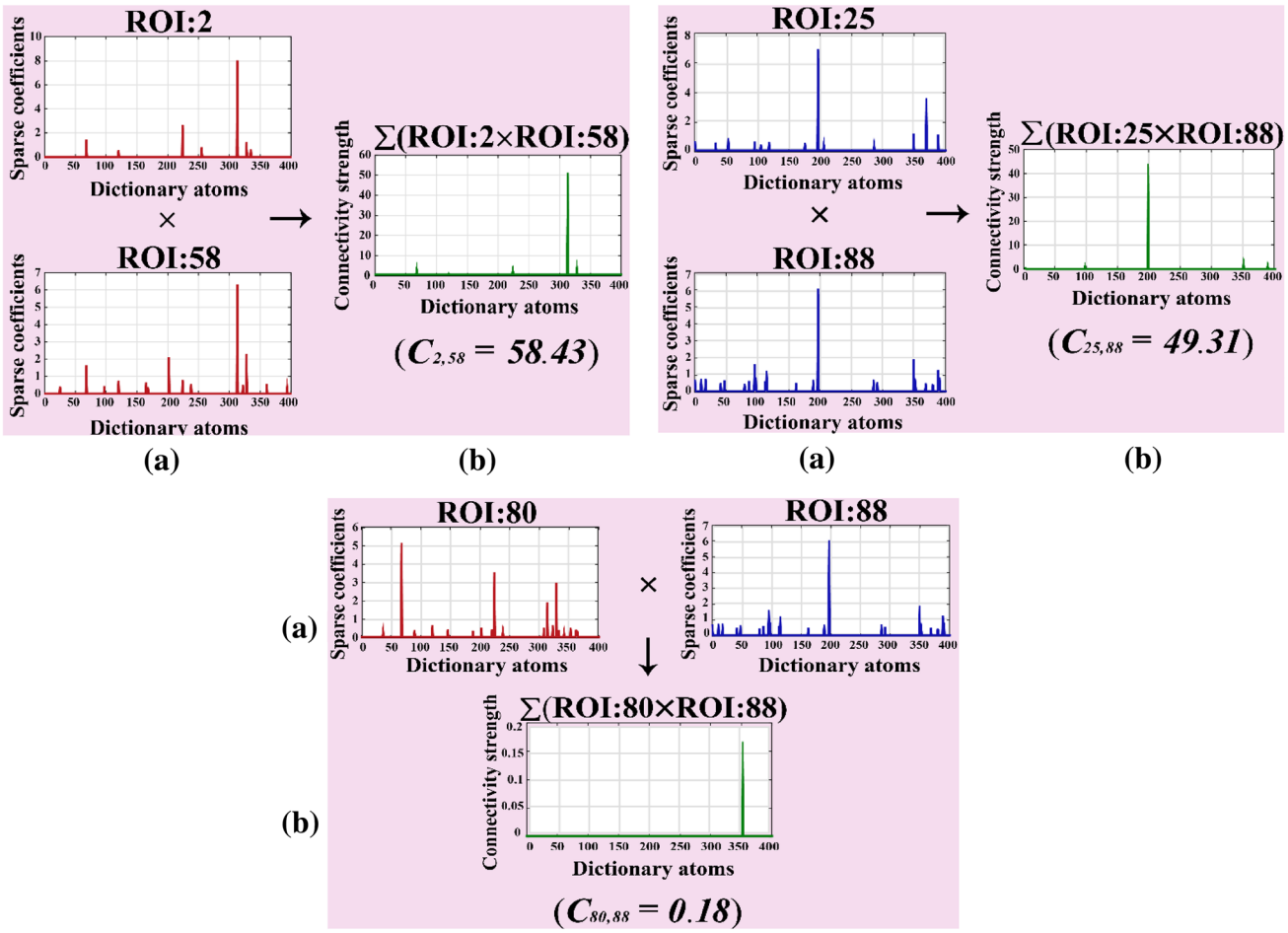

Fig. 1 Three examples of connectivity strength between the two brain regions which are computed through our proposed MSPW approach. The *x*-axis indicates the dictionary atoms ID, and the *y*-axis in (**a**) is the corresponding sparse coefficients. The *y*-axis in (**b**) indicates the pairwise connectivity strength

dissimilar regions in terms of activation type has a relatively lower value. As a result, each pairwise connection depends on the type of ROIs' activity that is specified based on sparse coefficients weight and associated representative atoms. Therefore, this method could preserved the modular structure of brain network by detecting the modules of regions that are densely interconnected with each other, while sparsely connected with regions in other modules.

In Fig. 1, the pairwise connectivity strength is computed based on our MSPW method, which is shown in three exemplars between the similar ROIs in terms of their activation type together and the heterogeneous areas.

Extraction of functional brain network properties

Overall, the following characteristics were examined in order to identify the discriminative topological properties between the two groups:

(1) We utilized the pairwise connectivity strengths of regions from weighted brain network, constructed based on our proposed MSPW method, to identify regions in each of their pairwise connections, which could make significant differences between the two groups. For this purpose, we applied the non-parametric Wilcoxon rank-sum test with correction by using false discovery rate (FDR) [57] of 10% for multiple comparisons over all connectivity strengths of regions. The MSPW-based functional connectivity network along with its topological structure are shown for one of the MS patients and one of the healthy individuals in Fig. 2.

(2) After the construction of the weighted connectivity network for each subject, we applied the proportional thresholding (PTh) [13] on resulted networks with the PTh values in the range of 0.1–0.50 to preserve 10–50% of the total number of network links (with a step size of 1%) and adjust the rest to zero. We used the proportional thresholding approach to match the link density across all subjects for the subsequent comparisons. In

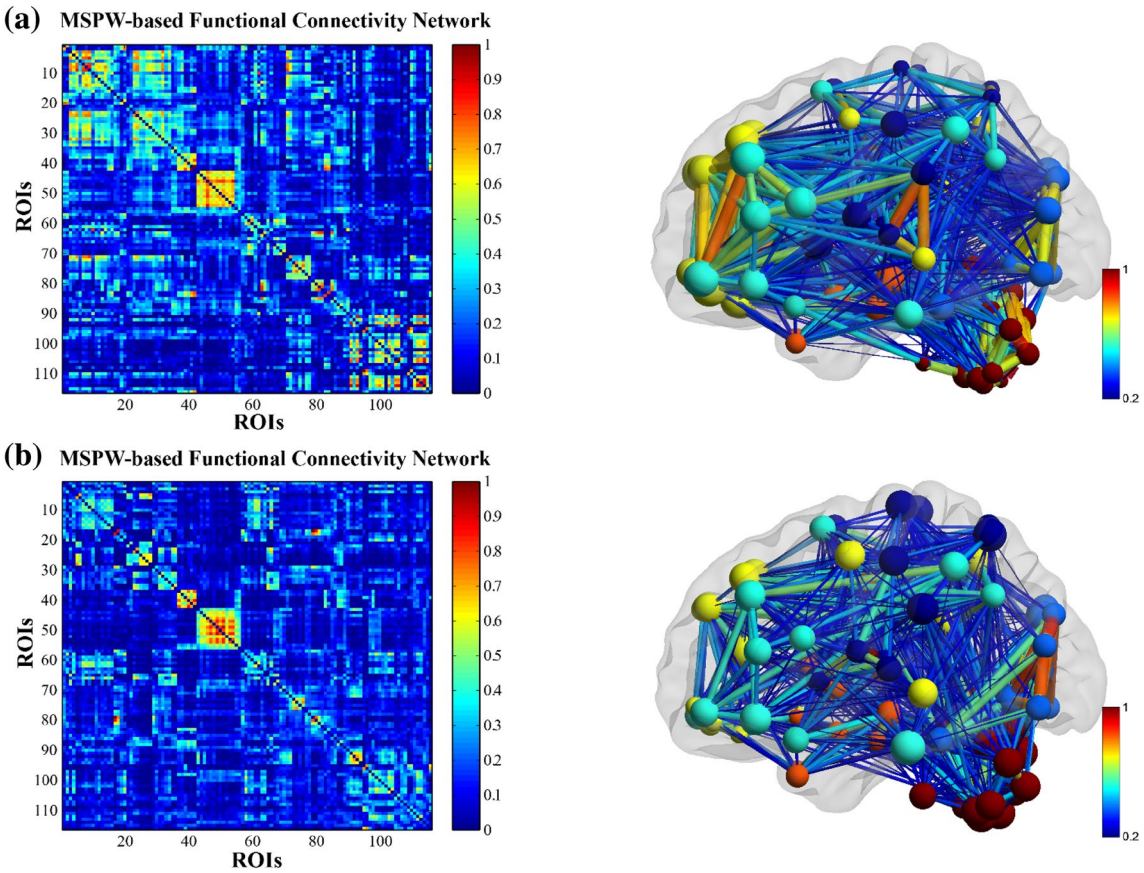

Fig. 2 Weighted functional connectivity network constructed based on our proposed MSPW method for all pairs of 116 ROIs, along with its topological structure including node degrees and connectivity strengths (in the right Figures: the width of each link determines the pairwise connectivity strength and the size of each node determines its degree): **a** for one of the patients with MS, **b** for one of the healthy individuals

addition, the selected PThs in the range of 0.1–0.50 can lead to the prevention of too sparse or dense connectivity networks in which either so important connections are removed or noisy and insignificant information is preserved. Then, we calculated a wide variety of graph-based characteristics from two different classes of global and local network properties through considering each thresholded functional network as a weighted graph:

- The global measures were extracted based on two aspects including functional segregation and integration. Mean clustering coefficient, mean local efficiency, modularity, and transitivity were defined as measures of functional segregation. The characteristic path length and global efficiency were described as measures of functional integration.
- The local graph properties are: clustering coefficient, local efficiency, eccentricity, and some measures

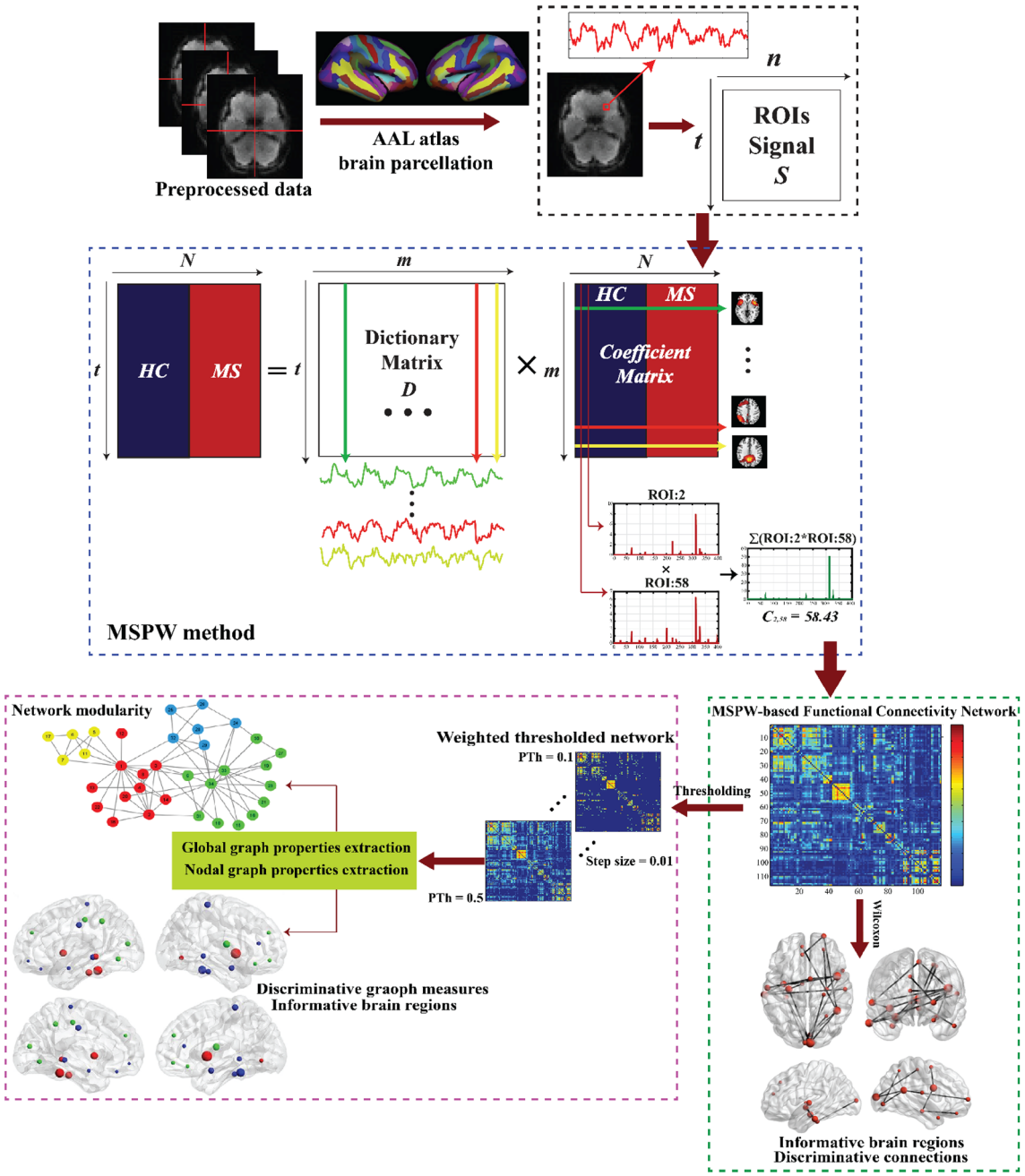

Fig. 3 Procedure for the proposed approach in this study

of centrality such as node strength, within-module degree, betweenness centrality, diversity centrality, eigenvector centrality, and participation coefficient.

We used the Brain Connectivity Toolbox (BCT) [15] to compute all the graph measures. More details about the methods and interpretation of these global and local graph measures are cited in [15].

Eventually, the non-parametric Wilcoxon rank-sum test was employed on all extracted global characteristics over all thresholded weighted networks (i.e., 41 graphs). In addition, we applied the Wilcoxon test on all nodal graph measures extracted from all thresholded weighted graphs to detect which brain regions had significantly changed in MS patients compared with those of the controls. We used the Wilcoxon test based on the corresponding resulted p-values, which was then corrected with a FDR of 5% for multiple comparisons. The overview of our proposed framework is illustrated in Fig. 3.

Results

Task-related and anti-task related dictionary atoms with the associated ROIs

In Fig. 4, all learned dictionary components are shown based on $E_{f_{PASAT}}$ and absolute values of their correlation with the task design, which were categorized into two types of task-related and anti-task-related components according to their positive and inverse correlations, respectively. Among these atoms, the components located in the top-right-hand corner of the Fig. 4 with both larger $E_{f_{PASAT}}$ and correlation scores were selected as the most responsive components to the task model. Accordingly, the two task related and five anti-task related components were identified from the common learned dictionary for all subjects. The AAL-based spatial distribution of each selected component was recognized through transforming the group-wise T-value results to the standard z-scores and thresholding at $Z > 1.65$. A total of 57 regions from the two groups were obtained, which correspond to these selected components. The selected dictionary atoms related to the task and anti-task with their corresponding temporal-frequency properties, and the associated regions are displayed in Figs. 5 and 6 for MS and HC groups separately. As can be seen, only 16 out of 57 regions are common between the two groups.

Topological properties of MSPW-based functional connectivity networks

We proposed a framework called MSPW for constructing the weighted functional connectivity networks by considering both sparse and modular structures, without neglecting the influence of other regions on pairwise connectivity strength.

Afterwards, we identified the discriminative topological characteristics from these MSPW-based functional connectivity networks, which were significantly different between the two groups of MS and control.

Statistical analysis on pairwise connectivity weights of regions

We identified the important connections of regions, which revealed significant differences between the two groups

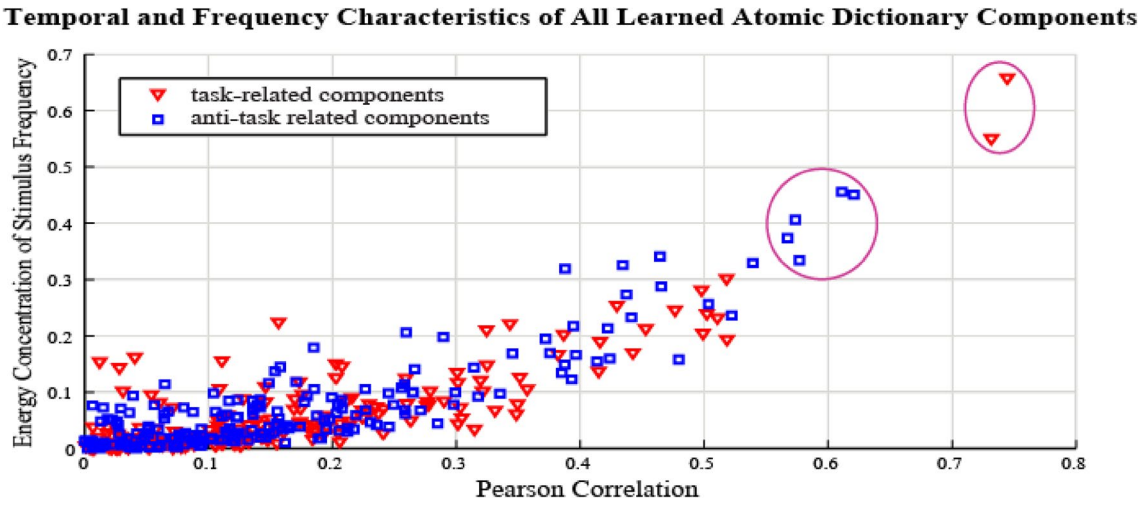

Fig. 4 All common learned dictionary atoms based on $E_{f_{PASAT}}$ and absolute values of their correlation with the task design. We selected the most responsive components to the task model, which are marked by drawing the circles around them

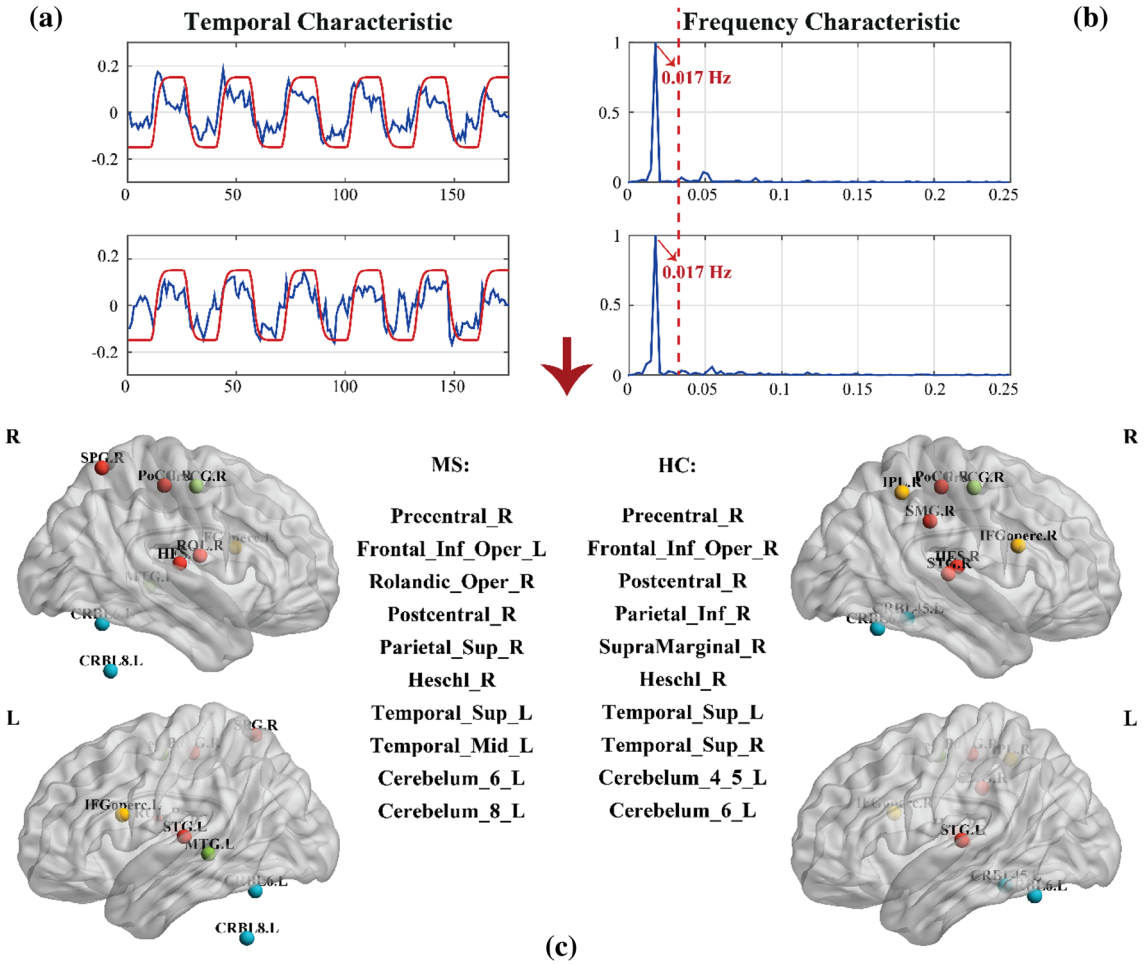

Fig. 5 The selected dictionary atoms related to the task with their corresponding **a** temporal characteristic: the red curves indicate the task paradigm. The *x*-axis is the temporal samples, and the *y*-axis shows the time course of each selected task-based atom which normalized to (-1, 1), **b** frequency characteristic: the *x*-axis is the frequency, and the corresponding energy normalizing to (0, 1) is indicated with *y*-axis, and **c** the associated regions in each group

based on Wilcoxon test results (FDR-corrected). Therefore, we could detect the informative brain regions that are related to these discriminative pairwise connectivity weights. These 33 significant connections are listed in Table 1, based on their corresponding regions.

These significant connections include the regions of bilateral fusiform gyrus, right heschl and superior temporal gyrus, left lingual gyrus and posterior cingulate, hippocampus and para hippocampal gyri, bilateral caudate, left amygdala, some parts of cerebellar and frontal gyrus. All discriminative regions are shown in Fig. 7. It is notable that almost half of these informative areas are included in regions, previously identified as the task-related or anti-task-related areas in this study in the first subsection of the Results.

Recent functional neuroimaging studies have found that the different parts of cerebellar are related to some cognitive functions like attention and mental imagery. Also, the heschl and superior temporal gyrus are mainly activated during auditory processing. The bilateral fusiform gyrus, hippocampus and para hippocampal, lingual, amygdala, and caudate are linked to memory, memory encoding and retrieval, semantic processing, memorization, the processing of memory, decision-making, identification and recognition. Moreover, the posterior cingulate cortex (PCC) is known as a central component of the default mode network (DMN) and is linked to memory, learning and attention (https://www.fmritools.com/kdb/grey-matter/index.html) [58].

The results of statistical analysis on functional connectivity strengths of regions demonstrate that the brain regions with these significant associated connections might be useful for the detection of cognitive dysfunctions in early MS patients.

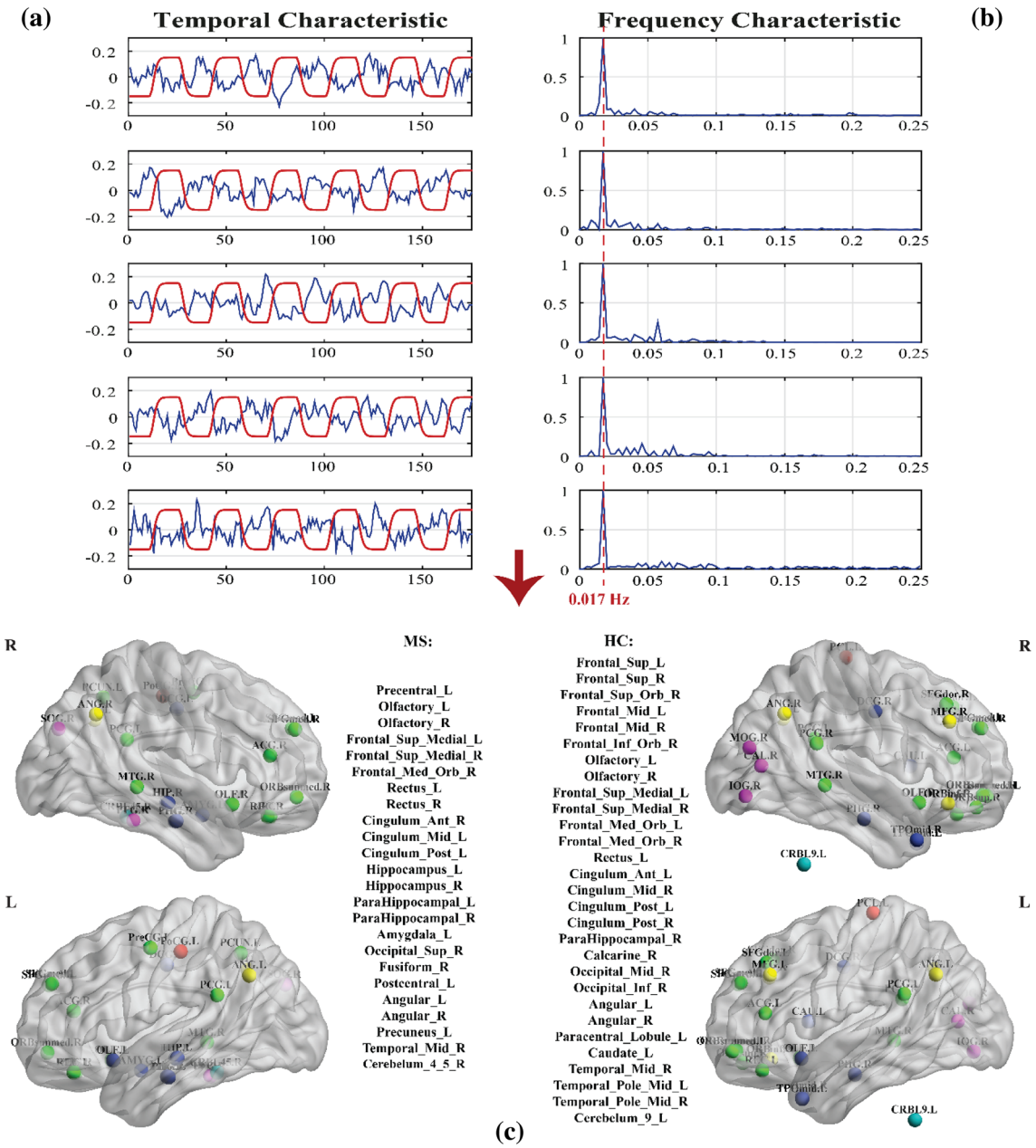

Fig. 6 The selected dictionary atoms related to the anti-task with their corresponding **a** temporal characteristic: the red curves indicate the task paradigm. The *x*-axis is the temporal samples, and the *y*-axis shows the time course of each selected anti-task-based atom which normalized to (-1, 1), **b** frequency characteristic: the *x*-axis is the frequency, and the corresponding energy normalizing to (0, 1) is indicated with *y*-axis, and **c** the associated regions in each group

Statistical analysis on graph-based measures

The results of statistical analysis on global features showed that only individual measure of modularity had significant alterations over nearly half of the range of PTh values between the two groups (Wilcoxon rank-sum test, FDR-corrected). Because our proposed method was established based on concept of modularity in the structure of brain networks, we expected the network modularity to indicate significant differences ($p < 0.05$, FDR-corrected) between the two groups. The standard error of mean of the obtained modularity values for all weighted networks in both groups are displayed in Fig. 8. As it is evident from Fig. 8, MS group display significantly lower values of modularity compared with those of the controls during cognitive task performance.

The results of statistical analysis on local graph measures are shown in Table 2. The results demonstrate each brain

Table 1 List of the brain ROIs with their most discriminative connections

ROI	MNI coordinate	AAL	The significant pairwise connectivity strengths	Lowest *p*-value
116	0, − 46, − 32	Vermis_10	ROIs: 17, 82 (task-related)	
			ROIs: 6, 10, 16, 22, 23, 24, 32, 37, 38, 40, 41, 56, 71 (anti-task-related)	0.001 (ROIs: 116, 71)
			ROIs: 5, 9, 14, 15, 18, 47, 51, 55, 57, 72, 73, 91, 100	
80	46, − 17, 10	Heschl_R (task-related)	ROIs: 105 (anti-task-related)	0.00079 (ROIs: 80, 105)
			ROIs: 104	
47	− 15, − 68, − 5	Lingual_L	ROIs: 16, 35 (anti-task-related)	0.00079 (ROIs: 47, 35)
56	34, − 39, − 20	Fusiform_R (anti-task-related)	ROI: 116	0.0014 (ROIs: 56, 116)
105	10, − 49, − 46	Cerebellum_9_L (anti-task-related)	ROI: 80 (anti-task-related)	0.00079 (ROIs: 105,80)
35	− 5, − 43, 25	Cingulum_Post_L (anti-task-related)	ROI: 46, 47	0.00079 (ROIs: 35, 47)

It was also determined which connection in each region had the lowest *p*-value (FDR-corrected). Regions were divided based on AAL atlas

MNI Montreal Neurological Institute space, *AAL* Automated Anatomical Labeling atlas

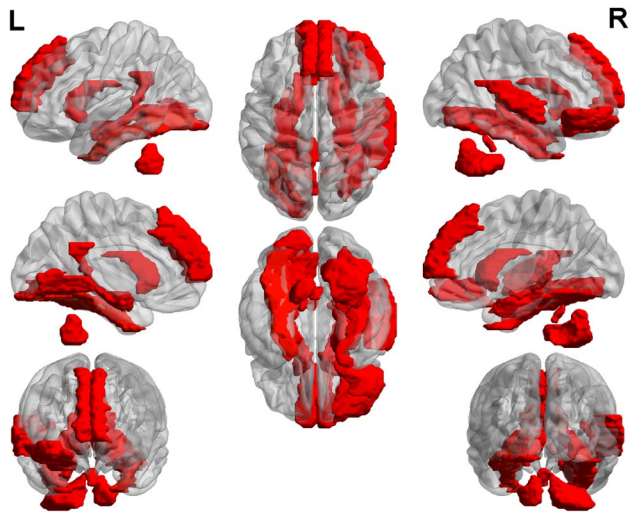

Fig. 7 Presentation of informative brain regions which could significantly distinguish between the two groups in their corresponding discriminative connections

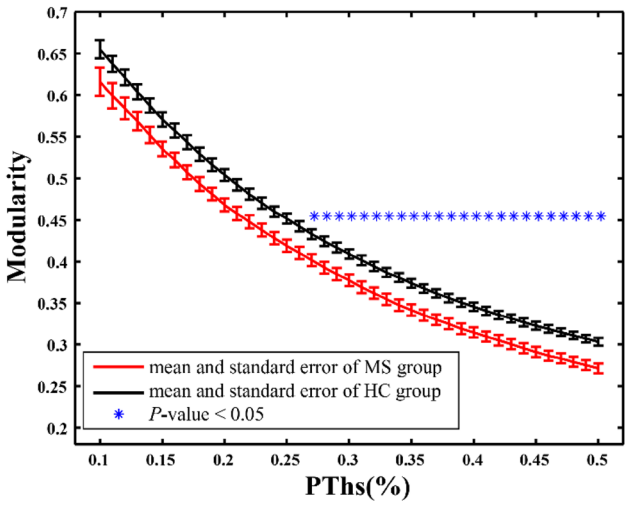

Fig. 8 Significant reduction in network modularity values for the weighted thresholded functional networks was determined for MS patients (red line) compared to control group (black line). Significant differences ($p < 0.05$, FDR-corrected) between the two groups are shown by blue stars

area that could possess the most number of significant differences between MS and HC among all associated nodal graph properties extracted from all the thresholded weighted networks. It can be seen from Table 2 that the brain areas such as right lingual, left medial orbital of superior frontal gyrus, and some parts of cerebellum show statistically significant differences between the two groups over more than 20 PTh values among the discriminative nodal measures of eigenvector centrality, node strength, eccentricity, and within-module degree.

We also calculated Spearman's correlation coefficients of clinical measures and cognitive performance with the most discriminative pairwise connections and graph features to evaluate the significance of any relationships between them. The connectivity strength of vermis_10 and left rolandic was significantly ($p < 0.05$, FDR-corrected) positively correlated with the verbal memory scores. There was a significant negative correlation between the eccentricity measure of vermis_1_2 and auditory attention scores at PThs from 0.21 to 0.5. Eigenvector centrality and node strength values of cerebelum_3_L also had significant negative correlation with the auditory attention scores in most PThs. Whereas clustering coefficient of right lingual showed a significant positive correlation with the auditory attention scores, this local measure was significantly negatively correlated with the disease duration. Figure S1 in Supplementary Material displays the scatter plots of the discriminative graph features

Table 2 The brain ROIs in corresponding discriminative local features which could significantly differentiate ($p < 0.05$, FDR-corrected) between the two groups over more than 20 of PTh values from 0.1 to 0.5 by step size of 0.01

Local graph measure	ROI	MNI coordinate	AAL	Lowest p-value
Eccentricity	109	1, − 39, − 20	Vermis_1_2	0.0005 (PTh = 0.21)
Eigenvector centrality	95	− 8, − 37, − 19	Cerebelum_3_L	0.0005 (PTh = 0.32)
Node strength	95	− 8, − 37, − 19	Cerebelum_3_L	0.0007 (PTh = 0.43)
Within-module degree	25	− 5, 54, − 7	Frontal_Med_Orb_L	0.0014 (PTh = 0.35)
Diversity centrality	25	− 5, 54, − 7	Frontal_Med_Orb_L	0.001 (PTh = 0.37)
Eigenvector centrality	109	1, − 39, − 20	Vermis_1_2	0.0023 (PTh = 0.12)
Node strength	109	1, − 39, − 20	Vermis_1_2	0.003 (PTh = 0.15)
Clustering coefficient	48	16, − 67, − 4	Lingual_R	0.001 (PTh = 0.21)
Eccentricity	95	− 8, − 37, − 19	Cerebelum_3_L	0.0062 (PTh = 0.27)

It is presented as the lowest p-value at its corresponding PTh in parenthesis for each nodal measure. Regions are divided based on AAL atlas

and pairwise connectivity weights which had significant positive or negative correlation with the clinical and cognitive measures.

Discussion

The main goal of this study was to propose a method for the construction of a functional connectivity network through the concept of brain network modular structure based on the sparse representation theory. The sparse signal representation obtained through learning a common over-complete dictionary from cognitive task-related fMRI data in order to identify the reliable markers for the detection of alterations in topological properties in early MS patients compared with the controls. Many neurological findings have supported the idea of the sparsity of the brain networks [22–24, 28–30]. In addition, modular structure is an important topological characteristic of the brain connectivity networks, which can provide information about the networks partitioning by investigating the inter-modular and intra-modular connectivity [38, 39]. Modularity is based on the concept that the functional connectivity between regions with similar specialized activities is strong and dense in the same module, whereas there is sparsely functional connectivity between regions from different modules.

Since the existence of structural damage can lead to the changes in topological properties of connectivity networks, we could identify these between-group differences using various topological measures by constructing the brain networks through considering both sparse and modular structures as important inherent characteristics of functional connectivity networks. The proposed MSPW method, with the examination of measures from different aspects of brain network, could recognized more significant connections in their corresponding ROIs and also important graph features that could distinguish MS patients from controls.

The present study integrated sparse representation, connectivity strength between the two regions by considering the influences of other regions, and the community structure for the construction of functional connectivity networks for the early assessment of cognitive-related alterations in MS disease. Wang et al. [22] reported high accuracy for classification of patients with depression and HC using sparse low-rank functional network model and graph features. Furthermore, Yu et al. [23] achieved more significant connections in the discrimination of patients with MCI and HC by proposing a model of "connectivity strength-weighted sparse group representation (WSGR)" for brain networks construction based on sparsity, connectivity weights derived from Pearson correlation, and group structure.

Modularity algorithm, through investigating the between-modular and within-modular connections, can describe the size and the way of combining densely interconnected areas in the same group to perform the specialized tasks and sparsely connected from different groups to transform the information [59, 60]. MS, as a disconnection disease, could affect the communication of the brain due to the presence of structural lesions [61]. In this regard, a significant reduction in modularity scores was observed in MS patients over all proportional thresholding values. The result of the proposed approach in combination with graph measures demonstrated that only single modularity feature (as a functional segregation measure) out of six extracted global measures indicated a high ability discriminating MS patients from the controls. This result is consistent with our previous study [13], which showed the modularity values computed from binary adjacency graphs constructed by Pearson correlation have significant differences over a wide range of PThs. By comparing the results of our proposed method with the Pearson's correlation, it could be seen that our model led to a clearer modular structure with larger modularity values for the constructed networks over different range of PTh values (for modularity values of the functional brain

network constructed by Pearson's correlation model and our proposed model see Fig. S2 in Supplementary Material).

Recent research studies of functional connectivity networks based on resting-state fMRI or a specific task performance have also reported the relevance of modularity to the cognitive dysfunctions in many different brain disorders [2, 13, 22, 58, 62, 63]. Liu et al. [58] utilized two measures of intra- and inter-module efficiency to evaluate the communication efficiency in early MS patients compared with the healthy controls. Their results showed a decreased inter-module efficiency between different functional connectivity networks in MS. Therefore, considering the importance of modular structure of brain networks, adding this property to network construction model could be closer to the real brain network, which could highlight the potential of network modularity score as a reliable marker to help the early identification of cognitive deficits.

The top four local graph measures of eigenvector centrality, node strength, eccentricity, and within-module degree could significantly identify the most number of between-group differences in brain networks by highlighting the ROIs' situation.

The influence of a node within the entire network is quantified by eigenvector centrality with the consideration of the quality of their connections. This measure allows us to detect the brain hubs [64–66]. In this regard, many studies in AD disease reported that the eigenvector centrality was an effective measure for the identification of main hubs, which could play an important role in detecting changes of cognitive symptoms in patients with AD [10, 21, 67, 68]. In addition, our findings are in line with a recent study, showing the crucial role of eigenvector centrality to define a major hub and relationship between the structural, functional and cognitive alterations in early MS patients [66].

The eccentricity measure determines the greatest distance between a certain ROI and all other areas in a network [69]. Our results are congruous with those of a study by Tewarie et al. [70] that revealed the nodal measure of eccentricity can significantly change in early RRMS in three frequency bands of theta, alpha2 and beta using resting-state magnetoencephalographic (MEG) data. It has also been reported by Hojjati et al. [68] that the eccentricity measure in the left fusiform was significantly different in converting MCI to AD.

The within-module degree denotes the intra-module connectivity of a node by considering the connections within community which it belongs, while participation centrality describes the relation between a node's connections within its own module and its connections to other nodes in different modules [15, 62]. Therefore, both measures were often compared with each other to denote the important nodes as hub regions, which can play a key role in the organization of brain network, particularly when damage has occurred. Several recent studies have emphasized the importance of hub regions for further understanding of brain disorders [21, 62, 71, 72]. Our results are consistent with those of a recent study by Haan et al. [62], indicating that these two mentioned properties are linked with the cognitive deficits. It is noteworthy that our findings obviously reflected the disrupted modular organization of brain networks in the early stages of MS disease for cognitive functions.

We also found a high capacity of node strength measure for separating MS patients from healthy controls, which is in line with the results of a recent study that detected significant covariations between cortical demyelination and white matter connectivity matrices like strength in the early MS patients [73].

The brain regions that significantly differentiated MS patients from controls in these top four discriminative nodal properties are corresponding to cerebelum_3_L, vermis_1_2, left medial orbital of superior frontal gyrus, lingual gyrus based on AAL atlas.

Several recent studies have reported the presence of gray matter (GM) lesions in early MS patients and identified cerebellum and hippocampus as the most affected regions among GM regions [74–76]. Although cerebellum is mainly related to motor control, some cognitive processes such as attention, high-level cognitive functions, and conflict adaptation have also been attributed to it (https://www.fmritools.com/kdb/grey-matter/index.html) [1, 10, 13, 42, 77–79]. An increased activity in cerebellum for healthy subjects during working memory performance have been observed in [79]. In addition, Petsas [42] indicated a significant inverse correlation between PASAT score and some areas including cerebellum in MS patients. Furthermore, although a linear growth of task-related activity in cerebellum was reported by Rocca et al. [77] for both groups of MS and HC during N-back load condition with increasing cognitive task difficulty, MS patients showed a lower increase of activity compared with the controls. Spiteri et al. [80] also revealed an association between decreased activation in executive regions like orbital part of left superior frontal gyrus and state of fatigue during the N-back task performance in MS patients compared with the controls.

Finally, we also found informative brain areas with significant differences between the two groups in terms of their pairwise connectivity strengths. As listed in Table 1, these most affected regions by cognitive impairments in MS were some parts of cerebellar and frontal gyrus, bilateral fusiform gyrus, right heschl and superior temporal gyrus, left lingual gyrus and posterior cingulate, hippocampus and para hippocampal gyri, bilateral caudate, left amygdala. Over the years, the neuroscientists have agreed that an important role of hippocampal functions is associated with memory. There are plenty of reports [81–92] that express any disruption in hippocampus can have severe effects on many domains

in cognition (https://www.fmritools.com/kdb/grey-matter/index.html). Moreover, it has been shown that early MS patients with hippocampal atrophy have significantly lower right hippocampal volume compared with the healthy controls, which can result in a decreased functional connectivity over hippocampus. It is worth noting that slight decreases of resting-state functional connectivity were also reported in patients with MS who did not have hippocampal volume abnormalities [81]. Consistent with the results of previous studies, Gamboa et al. [2] demonstrated that a community structure which belonged to the cerebellar regions in the control group was expanded through adding the hippocampus and para-hippocampal areas to the module in MS group during a cognitive task. Our results are in line with those of the previous studies, showing significant activation/deactivation of lingual and medial superior frontal gyrus in MS patients during PASAT and N-back tasks [77, 93, 94].

Consistent with the results of previous studies, the mentioned regions are involved in various aspects of cognitive dysfunctions for different neurological brain disorders. Accordingly, it seems that these discriminative brain regions could help us to improve our understanding of cognitive deficits in early stages of brain disorders such as MS disease (https://www.fmritools.com/kdb/grey-matter/index.html) [10, 13, 21, 58, 68, 77]. Since almost half of these significant brain areas were also specified as task/anti-task-related brain regions in this study, it can be suggested that the only assessment of functional connectivity between and within task and anti-task-related networks might guide us to find out more information about cognitive changes in topological organization in MS patients.

Conclusion

In this paper, we introduced a method for the construction of a functional connectivity network. The model was based on sparse representation obtained through learning a common dictionary from aggregated fMRI signals of MS patients and matched healthy controls during a specific cognitive task performance. We included two most important inherent characteristics of brain network, i.e. 'sparsity' and 'modular structure', into our method to construct functional networks and to clarify the brain topological organization in various conditions.

We investigated between-group differences by examining the pairwise connectivity strengths and graph-based topological properties, which derived from achieved weighted functional networks. Our results indicated that the network modularity measure was more effective than other global measures to reveal significant alterations of functional brain networks in MS and HC. We also identified the nodal level graph properties such as eigenvector centrality, eccentricity, node strength, and within-module degree, which showed a discrimination ability for the differentiation of the two groups. In addition, we detected a subset of informative brain regions corresponding to their discriminative connectivity weights and local graph properties, which are expected to be the most affected areas by cognitive problems in MS patients.

These results suggested that our proposed approach, the integration of sparsity, modular structure and pairwise connectivity strength in combination with graph theory, could serve for identification of the disrupted functional topological organization in MS patients suffering from cognitive deficits in the early stages of disease.

Acknowledgements This research has been financially supported by the Iran Neural Technology Research Center, Iran University of Science and Technology, Tehran, Iran under Grant 48. M.111194.

Compliance with ethical standards

Conflict of interest The authors declare that they have no conflict of interest.

Ethical approval All procedures performed in studies involving human participants were in accordance with the ethical standards of the institutional and/or national research committee and with the 1964 Helsinki declaration and its later amendments or comparable ethical standards.

Informed consent Informed consent was obtained from all individual participants included in the study.

References

1. Mainero C et al (2004) fMRI evidence of brain reorganization during attention and memory tasks in multiple sclerosis. Neuroimage 21(3):858–867
2. Gamboa OL et al (2014) Working memory performance of early MS patients correlates inversely with modularity increases in resting state functional connectivity networks. Neuroimage 94:385–395
3. Baysal Kıraç L, Ekmekçi Ö, Yüceyar N, Kocaman AS (2014) Assessment of early cognitive impairment in patients with clinically isolated syndromes and multiple sclerosis. Behav Neurol 2014:637694
4. Audoin B et al (2005) Magnetic resonance study of the influence of tissue damage and cortical reorganization on PASAT performance at the earliest stage of multiple sclerosis. Hum Brain Mapp 24(3):216–228
5. He BJ, Shulman GL, Snyder AZ, Corbetta M (2007) The role of impaired neuronal communication in neurological disorders. Curr Opin Neurol 20(6):655–660
6. Guye M, Bartolomei F, Ranjeva J-P (2008) Imaging structural and functional connectivity: towards a unified definition of human brain organization? Curr Opin Neurol 21(4):393–403
7. Bonavita S et al (2011) Distributed changes in default-mode resting-state connectivity in multiple sclerosis. Mult Scler J 17(4):411–422

8. Sporns O, Chialvo DR, Kaiser M, Hilgetag CC (2004) Organization, development and function of complex brain networks. Trends Cogn Sci 8(9):418–425
9. Supekar K, Menon V, Rubin D, Musen M, Greicius MD (2008) Network analysis of intrinsic functional brain connectivity in Alzheimer's disease. PLoS Comput Biol 4(6):e1000100
10. Khazaee A, Ebrahimzadeh A, Babajani-Feremi A (2016) Application of advanced machine learning methods on resting-state fMRI network for identification of mild cognitive impairment and Alzheimer's disease. Brain Imaging Behav 10(3):799–817
11. Onias H et al (2014) Brain complex network analysis by means of resting state fMRI and graph analysis: will it be helpful in clinical epilepsy? Epilepsy Behav 38:71–80
12. Eqlimi E et al (2014) Resting state functional connectivity analysis of multiple sclerosis and neuromyelitis optica using graph theory. In: XIII Mediterranean Conference on medical and biological engineering and computing 2013. Springer, pp 206–209
13. Ashtiani SNM et al (2018) Altered topological properties of brain networks in the early MS patients revealed by cognitive task-related fMRI and graph theory. Biomed Signal Process Control 40:385–395
14. Eguiluz VM, Chialvo DR, Cecchi G, Baliki M, Apkarian AV (2004) Scale-free brain functional networks. Neuroimage 22:2330
15. Rubinov M, Sporns O (2010) Complex network measures of brain connectivity: uses and interpretations. Neuroimage 52(3):1059–1069
16. Van Den Heuvel MP, Pol HEH (2010) Exploring the brain network: a review on resting-state fMRI functional connectivity. Eur Neuropsychopharmacol 20(8):519–534
17. Hampson M, Peterson BS, Skudlarski P, Gatenby JC, Gore JC (2002) Detection of functional connectivity using temporal correlations in MR images. Hum Brain Mapp 15(4):247–262
18. Power JD et al (2011) Functional network organization of the human brain. Neuron 72(4):665–678
19. Wee C-Y et al (2012) Resting-state multi-spectrum functional connectivity networks for identification of MCI patients. PLoS ONE 7(5):e37828
20. Murrough JW et al (2016) Reduced global functional connectivity of the medial prefrontal cortex in major depressive disorder. Hum Brain Mapp 37(9):3214–3223
21. Khazaee A, Ebrahimzadeh A, Babajani-Feremi A (2016) Classification of patients with MCI and AD from healthy controls using directed graph measures of resting-state fMRI. Behav Brain Res 30:339
22. Wang X, Ren Y, Zhang W (2017) Depression disorder classification of fmri data using sparse low-rank functional brain network and graph-based features. Comput Math Methods Med 2017:3609821
23. Yu R, Zhang H, An L, Chen X, Wei Z, Shen D (2017) Connectivity strength-weighted sparse group representation-based brain network construction for Mci classification. Hum Brain Mapp 38(5):2370–2383
24. McKeown MJ et al (1997) Analysis of fMRI data by blind separation into independent spatial components. Naval Health Research Center, San Diego
25. Esposito F et al (2002) Spatial independent component analysis of functional MRI time-series: to what extent do results depend on the algorithm used? Hum Brain Mapp 16(3):146–157
26. Rocca M et al (2010) Default-mode network dysfunction and cognitive impairment in progressive MS. Neurology 74(16):1252–1259
27. Roosendaal SD et al (2010) Resting state networks change in clinically isolated syndrome. Brain 133(6):1612–1621
28. Olshausen BA, Field DJ (1996) Emergence of simple-cell receptive field properties by learning a sparse code for natural images. Nature 381(6583):607
29. Daubechies I et al (2009) Independent component analysis for brain fMRI does not select for independence. Proc Natl Acad Sci 106(26):10415–10422
30. Lee K, Tak S, Ye JC (2011) A data-driven sparse GLM for fMRI analysis using sparse dictionary learning with MDL criterion. IEEE Trans Med Imaging 30(5):1076–1089
31. Stam C, Jones B, Nolte G, Breakspear M, Scheltens P (2007) Small-world networks and functional connectivity in Alzheimer's disease. Cereb Cortex 17(1):92–99
32. Fransson P (2005) Spontaneous low-frequency BOLD signal fluctuations: an fMRI investigation of the resting-state default mode of brain function hypothesis. Hum Brain Mapp 26(1):15–29
33. Huang S et al (2010) Learning brain connectivity of Alzheimer's disease by sparse inverse covariance estimation. NeuroImage 50(3):935–949
34. Wan J et al (2014) Identifying the neuroanatomical basis of cognitive impairment in Alzheimer's disease by correlation-and nonlinearity-aware sparse Bayesian learning. IEEE Trans Med Imaging 33(7):1475–1487
35. Lee Y-B et al (2016) Sparse SPM: group sparse-dictionary learning in SPM framework for resting-state functional connectivity MRI analysis. Neuroimage 125:1032–1045
36. Lee J, Jeong Y, and Ye JC (2013) Group sparse dictionary learning and inference for resting-state fMRI analysis of Alzheimer's disease. In: 2013 IEEE 10th International Symposium on biomedical imaging (ISBI). IEEE, pp. 540–543
37. Wee C-Y, Yap P-T, Zhang D, Wang L, Shen D (2014) Group-constrained sparse fMRI connectivity modeling for mild cognitive impairment identification. Brain Struct Funct 219(2):641–656
38. Newman ME (2004) Fast algorithm for detecting community structure in networks. Phys Rev E 69(6):066133
39. Newman ME (2006) Modularity and community structure in networks. Proc Natl Acad Sci 103(23):8577–8582
40. Wechsler D (1987) Wechsler memory scale-revised manual. Psychological Cooperation Inc., New York
41. Stroop J (1935) Studies of interference in serial verbal reactions. J Experiment Psychol 18:643–661
42. Petsas N (2012) Brain's functional connectivity alterations in multiple sclerosis: an fMRI investigation (Doctoral dissertation, Department of Phycology, Sapienza Università di Roma). http://hdl.handle.net/10805/2013
43. Smith SM, Jenkinson M, Woolrich MW, Beckmann CF, Behrens TE, Johansen-Berg H et al (2004) Advances in functional and structural MR image analysisand implementation as FSL. Neuroimage 23:S208–S219
44. Woolrich MW, Jbabdi S, Patenaude B, Chappell M, Makni S, Behrens T et al (2009) Bayesian analysis of neuroimaging data in FSL. Neuroimage 45(1):S173–S186
45. Jenkinson M, Beckmann CF, Behrens TE, Woolrich MW, Smith SM (2012) Fsl. Neuroimage 62(2):782–790
46. Smith SM (2002) Fast robust automated brain extraction. Hum Brain Mapp 17(3):143–155
47. Jenkinson M, Bannister P, Brady M, Smith S (2002) Improved optimization for therobust and accurate linear registration and motion correction of brain images. Neuroimage 17(2):825–841
48. Jenkinson M, Smith S (2001) A global optimisation method for robust affineregistration of brain images. Med Image Anal 5(2):143–156
49. Li Y, Namburi P, Yu Z, Guan C, Feng J, Gu Z (2009) Voxel selection in fMRI data analysis based on sparse representation. IEEE Trans Biomed Eng 56(10):2439–2451
50. Li Y, Long J, He L, Lu H, Gu Z, Sun P (2012) A sparse representation-based algorithm for pattern localization in brain imaging data analysis. PLoS ONE 7(12):e50332

51. Oikonomou VP, Blekas K, Astrakas L (2012) A sparse and spatially constrained generative regression model for fMRI data analysis. IEEE Trans Biomed Eng 59(1):58–67
52. Tzourio-Mazoyer N et al (2002) Automated anatomical labeling of activations in SPM using a macroscopic anatomical parcellation of the MNI MRI single-subject brain. Neuroimage 15(1):273–289
53. Mairal J, Bach F, Ponce J, Sapiro G (2010) Online learning for matrix factorization and sparse coding. J Mach Learn Res 11:19–60
54. Lv J et al (2015) Sparse representation of whole-brain fMRI signals for identification of functional networks. Med Image Anal 20(1):112–134
55. Friston KJ, Holmes AP, Worsley KJ, Poline JP, Frith CD, Frackowiak RS (1994) Statistical parametric maps in functional imaging: a general linear approach. Hum Brain Mapp 2(4):189–210
56. Van Schependom J, Gielen J, Laton J, D'hooghe MB, De Keyser J, Nagels G (2014) Graph theoretical analysis indicates cognitive impairment in MS stems from neural disconnection. NeuroImage 4:403–410
57. Genovese CR, Lazar NA, Nichols T (2002) Thresholding of statisticalmaps in functional neuroimaging using the false discovery rate. Neuro-image 15:870–878
58. Liu Y, Duan Y, Dong H, Barkhof F, Li K, Shu N (2018) Disrupted module efficiency of structural and functional brain connectomes in clinically isolated syndrome and multiple sclerosis. Front Hum Neurosci 12:138
59. Girvan M, Newman ME (2002) Community structure in social and biological networks. Proc Natl Acad Sci 99(12):7821–7826
60. Danon L, Diaz-Guilera A, Duch J, Arenas A (2005) Comparing community structure identification. J Stat Mech 2005(09):P09008
61. Catani M, Jones DK (2005) Perisylvian language networks of the human brain. Ann Neurol 57(1):8–16
62. de Haan W, van der Flier WM, Koene T, Smits LL, Scheltens P, Stam CJ (2012) Disrupted modular brain dynamics reflect cognitive dysfunction in Alzheimer's disease. Neuroimage 59(4):3085–3093
63. Buldú JM et al (2011) Reorganization of functional networks in mild cognitive impairment. PLoS ONE 6(5):e19584
64. Bonacich P (1972) Factoring and weighting approaches to status scores and clique identification. J Math Sociol 2(1):113–120
65. Bonacich P (2007) Some unique properties of eigenvector centrality. Soc Netw 29(4):555–564
66. Hardmeier M et al (2012) Cognitive dysfunction in early multiple sclerosis: altered centrality derived from resting-state functional connectivity using magneto-encephalography. PLoS ONE 7(7):e42087
67. Binnewijzend MA et al (2014) Brain network alterations in Alzheimer's disease measured by Eigenvector centrality in fMRI are related to cognition and CSF biomarkers. Hum Brain Mapp 35(5):2383–2393
68. Hojjati SH, Ebrahimzadeh A, Khazaee A, Babajani-Feremi A, Initiative ASDN (2017) Predicting conversion from MCI to AD using resting-state fMRI, graph theoretical approach and SVM. J Neurosci Methods 282:69–80
69. Harris JM, Hirst JL, Mossinghoff MJ (2008) Combinatorics and graph theory. Springer, New York
70. Tewarie P et al (2014) Functional brain network analysis using minimum spanning trees in multiple sclerosis: an MEG source-space study. Neuroimage 88:308–318
71. Menon V (2013) Developmental pathways to functional brain networks: emerging principles. Trends Cogn Sci 17(12):627–640
72. de Haan W, Mott K, van Straaten EC, Scheltens P, Stam CJ (2012) Activity dependent degeneration explains hub vulnerability in Alzheimer's disease. PLoS Comput Biol 8(8):e1002582
73. Mangeat G et al (2018) Changes in structural network are associated with cortical demyelination in early multiple sclerosis. Hum Brain Mapp 39:2133
74. Vercellino M, Plano F, Votta B, Mutani R, Giordana MT, Cavalla P (2005) Grey matter pathology in multiple sclerosis. J Neuropathol Exp Neurol 64(12):1101–1107
75. Lucchinetti CF et al (2011) Inflammatory cortical demyelination in early multiple sclerosis. N Engl J Med 365(23):2188–2197
76. Gilmore CP, Donaldson I, Bö L, Owens T, Lowe J, Evangelou N (2009) Regional variations in the extent and pattern of grey matter demyelination in multiple sclerosis: a comparison between the cerebral cortex, cerebellar cortex, deep grey matter nuclei and the spinal cord. J Neurol Neurosurg Psychiatry 80(2):182–187
77. Rocca MA et al (2014) Functional correlates of cognitive dysfunction in multiple sclerosis: a multicenter fMRI Study. Hum Brain Mapp 35(12):5799–5814
78. Tüdös Z, Hok P, Hrdina L, Hluštík P (2014) Modality effects in paced serial addition task: Differential responses to auditory and visual stimuli. Neuroscience 272:10–20
79. Spiteri S, Hassa T, Claros-Salinas D, Schoenfeld M, and Dettmers C (2016) Functional MRI changes illustrating cognitive fatigue in patients with multiple sclerosis, vol 25. Rehabilitationswissenschaftliches Kolloquium, p. 370.
80. Cabeza R, Nyberg L (2000) Imaging cognition II: an empirical review of 275 PET and fMRI studies. J Cogn Neurosci 12(1):1–47
81. Roosendaal SD et al (2010) Structural and functional hippocampal changes in multiple sclerosis patients with intact memory function. Radiology 255(2):595–604
82. Cruz-Gómez Á, Belenguer-Benavides A, Martinez-Bronchal B, Fittipaldi-Márquez M, Forn C (2016) Structural and functional changes of the hippocampus in patients with multiple sclerosis and their relationship with memory processes. Rev Neurol 62(1):6–12
83. Eichenbaum H, Dudchenko P, Wood E, Shapiro M, Tanila H (1999) The hippocampus, memory, and place cells: is it spatial memory or a memory space? Neuron 23(2):209–226
84. Squire LR (1992) Memory and the hippocampus: a synthesis from findings with rats, monkeys, and humans. Psychol Rev 99(2):195
85. Suarez AN, Noble EE, Kanoski SE (2019) Regulation of memory function by feeding-relevant biological systems: following the breadcrumbs to the hippocampus. Front Mol Neurosci 12:101
86. Moscovitch M, Cabeza R, Winocur G, Nadel L (2016) Episodic memory and beyond: the hippocampus and neocortex in transformation. Annu Rev Psychol 67:105–134
87. Ragland JD, Layher E, Hannula DE, Niendam TA, Lesh TA, Solomon M, Carter CS, Ranganath C (2017) Impact of schizophrenia on anterior and posterior hippocampus during memory for complex scenes. NeuroImage 13:82–88
88. Moscovitch M, Nadel L, Winocur G, Gilboa A, Rosenbaum RS (2006) The cognitive neuroscience of remote episodic, semantic and spatial memory. Curr Opin Neurobiol 16(2):179–190
89. Burgess N, Maguire EA, O'Keefe J (2002) The human hippocampus and spatial and episodic memory. Neuron 35(4):625–641
90. Klur S, Muller C, Pereira de Vasconcelos A, Ballard T, Lopez J, Galani R, Certa U, Cassel JC (2009) Hippocampal-dependent spatial memory functions might be lateralized in rats: an approach combining gene expression profiling and reversible inactivation. Hippocampus 19(9):800–816
91. Geurts JJ, Bö L, Roosendaal SD, Hazes T, Daniëls R, Barkhof F, Witter MP, Huitinga I, van der Valk P (2007) Extensive

hippocampal demyelination in multiple sclerosis. J Neuropathol Exp Neurol 66(9):819–827
92. Zhou Y, Dougherty JH Jr, Hubner KF, Bai B, Cannon RL, Hutson RK (2008) Abnormal connectivity in the posterior cingulate and hippocampus in early Alzheimer's disease and mild cognitive impairment. Alzheimer's Dementia 4(4):265–270
93. Leonardi N, Richiardi J, and Van De Ville D (2013) Functional connectivity eigennetworks reveal different brain dynamics in multiple sclerosis patients. In: 2013 IEEE 10th International Symposium on biomedical imaging (ISBI). IEEE, pp 528–531
94. Forn C et al (2006) Cortical reorganization during PASAT task in MS patients with preserved working memory functions. Neuroimage 31(2):686–691